



# Lawrence Berkeley Laboratory

UNIVERSITY OF CALIFORNIA

## Materials Sciences Division

Submitted to Journal of the American Ceramic Society

### Sintering of Nanophase $\gamma$ - $\text{Al}_2\text{O}_3$ Powder

S.J. Wu, L.C. De Jonghe, and M.N. Rahaman

August 1995



REFERENCE COPY |  
Does Not |  
Circulate |  
Bldg. 50 Library. |  
COPY 1

LBL-37596

## **DISCLAIMER**

This document was prepared as an account of work sponsored by the United States Government. While this document is believed to contain correct information, neither the United States Government nor any agency thereof, nor the Regents of the University of California, nor any of their employees, makes any warranty, express or implied, or assumes any legal responsibility for the accuracy, completeness, or usefulness of any information, apparatus, product, or process disclosed, or represents that its use would not infringe privately owned rights. Reference herein to any specific commercial product, process, or service by its trade name, trademark, manufacturer, or otherwise, does not necessarily constitute or imply its endorsement, recommendation, or favoring by the United States Government or any agency thereof, or the Regents of the University of California. The views and opinions of authors expressed herein do not necessarily state or reflect those of the United States Government or any agency thereof or the Regents of the University of California.

Sintering of Nanophase  $\gamma$ -Al<sub>2</sub>O<sub>3</sub> Powder

Shun J. Wu and Lutgard C. De Jonghe

Department of Materials Science and Mineral Engineering  
University of California  
Berkeley, California 94720

And

Materials Sciences Division  
Lawrence Berkeley National Laboratory  
University of California  
Berkeley, California 94720

Mohamed N. Rahaman

Department of Ceramic Engineering  
University of Missouri-Rolla  
Rolla, Missouri 65401

August 1995

# Sintering of Nanophase $\gamma$ -Al<sub>2</sub>O<sub>3</sub> Powder

Shun J. Wu\*<sup>+</sup> and Lutgard C. De Jonghe\*

Materials Sciences Division, Lawrence Berkeley Laboratory, and Department of Materials Science and Mineral Engineering, University of California, Berkeley, CA 94720

Mohamed N. Rahaman\*

University of Missouri-Rolla, Department of Ceramic Engineering, Rolla MO 65401

## Abstract

The sintering of an ultra-fine  $\gamma$ -Al<sub>2</sub>O<sub>3</sub> powder (particle size  $\approx$ 10-20 nm) prepared by an inert gas condensation method was investigated in air at a constant heating rate of 10 °C/min. Measurable shrinkage commenced at  $\approx$ 1000 °C and showed a region of very rapid sintering between  $\approx$ 1125 and 1175 °C followed by a transition to a much reduced sintering rate at higher temperatures. The transition in sintering behavior was related to the microstructural changes accompanying the crystallographic transformation of the powder system to the  $\alpha$ -Al<sub>2</sub>O<sub>3</sub> phase. Starting from an initial density of  $\approx$ 0.60 relative to the theoretical value, the powder compact reached a relative density of 0.82 after sintering to 1350 °C. The effects of prolonged annealing at temperatures below 1000 °C, seeding with fine-grained  $\alpha$ -Al<sub>2</sub>O<sub>3</sub> and doping with MgO on the sintering characteristics were investigated. The incorporation of a step involving the rapid heating of the powder to  $\approx$ 1300 °C prior to compaction (which resulted in the transformation to  $\alpha$ -Al<sub>2</sub>O<sub>3</sub>) provided the most beneficial process for increasing the density during sintering.

---

\*Member, the American Ceramic Society.

<sup>+</sup>Present address: Applied Materials, 3050 Bowers Ave., Santa Clara, CA 95054

Supported by the Division of Materials Sciences, Office of Basic Energy Sciences, U. S. Department of Energy, under Contract No. DE-AC03-76SF00098.

## I. Introduction

Ultrafine powders with particle sizes less than 50-100 nm, referred to as nanocrystalline or nanophase powders [1], can have significantly enhanced sintering rates and decreased sintering temperatures compared to coarse-grained (micron-sized) powders. [1-3]. They may allow the formation of novel materials that cannot be produced by the sintering of their coarse-grained counterparts. One class of such novel materials includes those with high density and ultrafine grain size. Another class includes those that undergo polymorphic transformations or chemical reactions at higher temperatures. In this case, the fast sintering rates of ultrafine powders can be used in the production of solids consisting of low-temperature polymorphs or solids with unreacted phases.

The present work involved an investigation of the sintering characteristics of an ultrafine  $\text{Al}_2\text{O}_3$  powder prepared by the inert gas condensation technique described by Gleiter et al [4] and by Eastman et al [1]. Briefly, in this technique, a metal (e.g., Al) is first evaporated in a chamber containing a He atmosphere. Fine particles condense from the vapor and are collected on a cold shroud. The chamber is then evacuated and filled with  $\text{O}_2$  which promotes rapid oxidation of the powder. Finally, the powder is scraped off the shroud.

$\text{Al}_2\text{O}_3$  materials produced at relatively low temperatures, such as those derived from gelatinous boehmite and other hydrous oxides of alumina, undergo a number of phase transformations prior to the formation of the  $\alpha$ -phase. The materials generally have a characteristic sintering behavior consisting of a region of very fast sintering rates between  $\approx 1000$  and  $1200^\circ\text{C}$  followed by a transition to much lower sintering rates at higher temperatures [5]. The transition in sintering behavior is related to the transformation from  $\theta$  to  $\alpha$ - $\text{Al}_2\text{O}_3$  which occurs rapidly in fine-grained  $\theta$ - $\text{Al}_2\text{O}_3$ . The vermicular microstructure consisting of an extensive network of large pores which develops during the transformation requires relatively high temperatures ( $\approx 1600^\circ\text{C}$ ) for the achievement of high density. Because of the densification difficulties caused by the transformation,  $\text{Al}_2\text{O}_3$  bodies are normally fabricated by the compaction and sintering of  $\alpha$ - $\text{Al}_2\text{O}_3$  powders. However, it has been shown that seeding of

boehmite gels with fine  $\alpha$ -Al<sub>2</sub>O<sub>3</sub> particles leads to an increase in the transformation kinetics and a lowering of the transformation temperature [6]. With the use of the seed particles, a fine-grained microstructure of  $\alpha$ -Al<sub>2</sub>O<sub>3</sub> develops which can be sintered to nearly full density at  $\approx 1200$  °C.

## II. Experimental Procedure

The Al<sub>2</sub>O<sub>3</sub> powder used in the experiments was provided by Nanophase Technologies Corp., Darien, IL. Transmission electron microscopy showed that the particles were almost spherical with a fairly wide distribution in size (Fig. 1). X-ray analysis revealed that the powder consisted predominantly of the  $\gamma$ -phase and a small amount of the  $\theta$ -phase. Within the limits of detection of the diffractometer ( $\approx 1$  wt %), no free Al was present.

Powder compacts (5 mm in diameter by 2 mm) were formed by uniaxial pressing in a die ( $\approx 20$  MPa) followed by cold isostatic pressing ( $\approx 1$  GPa). The compacts had a density of  $\approx 2.3$  g/cm<sup>3</sup>, which corresponded to  $\approx 63\%$  of the theoretical density of the solid ( $\approx 3.66$  g/cm<sup>3</sup>) as stated by the manufacturer. However, for consistency, the densities of the compacts will henceforth be determined relative to the theoretical value of the  $\alpha$ -phase (3.96 g/cm<sup>3</sup>).

Sintering of the powder compacts was performed in air at 10 °C/min to 1350 °C in a dilatometer that allowed continuous monitoring of the shrinkage. The temperature of 1350 °C represents roughly the maximum temperature capability of the instrument. The effect of prolonged annealing of the powder compacts at lower temperatures on the subsequent sintering was investigated. In the experiments, the powder compacts were heated at 10 °C/min to fixed temperatures between 500 and 900 °C and annealed for up to 72 h, after which they were heated at 10 °C/min to 1350 °C. As a comparison, the effect of converting the powder to the  $\alpha$ -phase prior to compaction and sintering was investigated. In these experiments, the loose powder was placed in a platinum crucible and heated rapidly (in 5 min) to 1300 °C after which it was quenched to room temperature. Following light grinding in an agate mortar and pestle, the powder was compacted and sintered as described earlier.

The effects of seeding with  $\alpha$ -Al<sub>2</sub>O<sub>3</sub> particles or doping with MgO on the sinterability of the as-received powder were also investigated. For the seeding experiments, the powder was dispersed in distilled water and mixed with 5 wt % of  $\alpha$ -Al<sub>2</sub>O<sub>3</sub> particles (AKP-53; Sumitomo Chemical Co. Ltd.). The mixture was disrupted with an ultrasonic probe to break up any soft agglomerates and stirred until it was dry. The dried powder was ground lightly in an agate mortar and pestle prior to compaction and sintering. Doping with MgO (Mg:Al atomic ratio = 250 ppm) was performed by dissolving the required amount of Mg(NO<sub>3</sub>)<sub>2</sub>·6H<sub>2</sub>O (EM Science, Gibbstown, NJ) in distilled water and dispersing the Al<sub>2</sub>O<sub>3</sub> powder in the solution. The mixture was stirred until it was dried, calcined for 2 h at 800 °C and ground lightly in an agate mortar and pestle. The doped powder was compacted and sintered under the conditions described earlier.

The crystalline phases present in the powders and sintered materials were determined by X-ray diffraction using Cu K $\alpha$  radiation at a scan rate of 2° 2 $\theta$  per minute. The microstructure of the sintered materials was observed by high resolution scanning electron microscopy of fractured surfaces.

### III. Results and Discussion

The sinterability of the compacts formed from the powder as received from the manufacturer (the "as-received powder") is shown in Fig. 2, where the shrinkage,  $\Delta L/L_0$ , and the relative density,  $\rho$ , are plotted as a function of temperature, T. ( $\Delta L = L_0 - L$ , where  $L_0$  is the initial sample length and L is the instantaneous sample length.) The temperature at which measurable shrinkage begins ( $\approx 1000$  °C) is comparable to that observed for compacts of submicron  $\alpha$ -Al<sub>2</sub>O<sub>3</sub> powders (e.g., AKP-53; Sumitomo Chemical Co. Ltd.). A distinctive feature of the sintering kinetics, however, is the extremely rapid shrinkage between  $\approx 1125$  and 1175 °C followed by a transition to a significantly reduced sintering rate. The value of  $\rho$  at the end of the sintering run (1350 °C) was only 0.82. The transition in the sintering kinetics at  $\approx 1175$  °C shows trend similar to those described earlier for Al<sub>2</sub>O<sub>3</sub> derived from gelatinous boehmite and other hydrous oxides of alumina. Isothermal sintering at  $\approx 1150$  °C (i.e., at the temperature of maximum sintering rate)

failed to produce any significant increase in the density obtained in constant heating rate sintering to 1350 °C.

The transition in the sintering behavior observed in Fig. 2 correlates with the polymorphic transformation of the powder to the  $\alpha$ -phase. Figure 3 shows the X-ray diffraction patterns of the powder compact soon before (1100 °C) and soon after (1200 °C) the transition in the sintering rate. A different powder compact was used for each run. At 1100 °C, the powder compact consists of a mixture of the  $\gamma$  and  $\theta$  phases but contains almost no  $\alpha$ -phase. However, at 1200 °C, the transformation to the  $\alpha$ -phase is essentially completed.

Figure 4 shows SEM micrographs of the fractured surfaces of the powder compacts sintered to 1100, 1200, and 1350 °C. At 1100 °C, the microstructure shows fairly uniform packing with almost rounded grains [Fig. 4(a)]. While the linear shrinkage of the compact at this temperature was only  $\approx 1\%$ , appreciable coarsening has occurred. The grain sizes are in the range of 25 to 50 nm, which corresponds to 2-3 times the initial particle size. Between 1100 and 1200 °C, the microstructure changes drastically [Fig. 4(b)]. Rapid coarsening and the development of a vermicular microstructure of elongated pores and grains have occurred. At 1350 °C, the microstructure [Fig. 4(c)] is a significantly coarsened version of that produced after the transformation to the  $\alpha$ -phase.

Figure 5 shows the shrinkage kinetics of compacts formed from the powder heated rapidly to 1300 °C prior to compaction [curve (a) in Fig. 5], the powder doped with MgO [curve (c)], and the powder seeded with fine  $\alpha$ -Al<sub>2</sub>O<sub>3</sub> particles [curve (d)]. For comparison, the data for the compact formed from the as-received powder is also shown [curve (b)]. For the compact formed from the as-received powder, the inclusion of an annealing step (10-72 h at 500, 700 or 900 °C) in the heating schedule did not influence the sintering kinetics significantly and the results are omitted from Fig. 5 to maintain clarity. The data for the seeded powder do not show the fairly sharp transition in the sintering kinetics at  $\approx 1150$  °C as observed earlier for the as-received powder. Furthermore, the onset of measurable shrinkage occurs at a lower temperature ( $\approx 975$  °C) than for the as-received powder ( $\approx 1025$  °C). The absence of the transition coupled

with the lowering of the onset for sintering indicates that the  $\alpha$ - $\text{Al}_2\text{O}_3$  seed particles influenced the transformation kinetics. However, an important aspect of the data is that the shrinkage kinetics are significantly lower than those for the as-received powder. For the MgO-doped powder, the sintering kinetics are also significantly lower than those for as-received powder. Furthermore, the dopant appears to have no significant effect on the microstructural evolution because the shape of the sintering curve shows trends that are similar to those observed for the as-received powder.

Compared to the as-received powders, the only significant difference in the processing route for the seeded powders and the doped powders is the step involving the mixing and subsequent drying. Indeed, it was found that if the as-received powder was given the same processing treatment as the doped powder (but without the dopant), the shrinkage kinetics were nearly the same as those of the doped powder. The data indicate that exposure to water and the subsequent drying have a detrimental effect on the sintering of the powders. As outlined earlier, the  $\text{Al}_2\text{O}_3$  powder used in this work was synthesized by the inert gas condensation technique of Gleiter et al [4] and involves the oxidation of fine Al particles in a dry chamber. It can be expected that on removal from the chamber, the surfaces of the powder will be partially hydrolyzed due to exposure to moisture from the atmosphere. In the experiments, further hydrolysis will occur during the mixing stage. During drying, condensation of hydroxyl groups can lead to strong bonds between the particles. The dried powder would therefore be expected to consist of a mass of hard agglomerates. Compared to the as-received powder, the reduction in the sinterability of the seeded powder and of the doped powder is attributed to the effects of enhanced agglomeration produced during the drying of the powder slurry. The elimination of the drying process, through the use of wet consolidation methods (e.g., slip casting or pressure casting) is likely to produce more beneficial sintering characteristics. However, because of their ultrafine size, the wet consolidation of nanocrystalline powders may require considerably more care than that employed for micron-sized powders.

The data of Fig. 5 also show that the compact formed from the powder heated rapidly to 1300 °C (to cause transformation to the  $\alpha$ -phase) undergoes the largest shrinkage. The relative density of the compact after sintering to 1350 °C was 0.95. This value of the relative density, while higher than that for the as-received powder (0.82), is still only roughly comparable to that obtained with a submicron  $\alpha$ -Al<sub>2</sub>O<sub>3</sub> powder (e.g., AKP-53; Sumitomo Chemical Co. Ltd.) consolidated by slip casting, and sintered under identical conditions. However, the results point to a possible route for alleviating the sintering difficulties of the Al<sub>2</sub>O<sub>3</sub> powder prepared by the inert gas condensation technique. In the present work, the loose powder was heated in a platinum crucible so that some agglomeration can be expected to occur. In the inert gas condensation technique, the incorporation of an additional gas suspension step after the oxidation stage, in which the powder is heated to convert individual Al<sub>2</sub>O<sub>3</sub> particles to individual particles of the  $\alpha$ -phase, is expected to prevent agglomeration of the powder and provide the beneficial sintering characteristics of an ultrafine  $\alpha$ -Al<sub>2</sub>O<sub>3</sub> powder.

#### IV. Conclusions

The sintering characteristics of ultrafine Al<sub>2</sub>O<sub>3</sub> powder prepared by the inert gas condensation technique show trends that are comparable to those of aluminas produced from boehmite gels and other hydrous and transitional oxides of aluminum. Measurable shrinkage commences at  $\approx$ 1000 °C and a region of very rapid sintering between  $\approx$ 1125 and 1175 °C is followed by a transition to a much reduced sintering rate at higher temperatures. The transition in sintering behavior is related to the microstructural changes accompanying the crystallographic transformation of the powder system to the  $\alpha$ -Al<sub>2</sub>O<sub>3</sub> phase.

Dispersion in water followed by drying leads to a significant reduction of the sinterability of the powder. The origins of the reduced sinterability appear to lie in the formation of strong bonds between the particles during the drying process. Because of the detrimental effect of exposure to water, the use of seeding with  $\alpha$ -Al<sub>2</sub>O<sub>3</sub> particles or doping with MgO is ineffective for controlling the microstructural evolution and improving the densification of the powder

compact. The inclusion of an additional step in the inert gas condensation technique in which the powder is heated to convert individual  $\text{Al}_2\text{O}_3$  particles to individual particles of the  $\alpha$ -phase may provide a method for improving the low temperature sinterability of the powder.

## References

1. J. A. Eastman, Y. X. Liao, A. Narayanasamy, and R. W. Siegel, "Processing and Properties of Nanophase Oxides," in Processing Science of Advanced Ceramics, I. A. Aksay, G. McVay, and D. Ulrich, Eds., Mater. Res. Soc. Symp. Proc., **155** 255-66 (1989).
2. H. Hahn, J. Logas, and R. S. Averback, "Sintering Characteristics of Nanocrystalline  $\text{TiO}_2$ ," J. Mater. Res., **5** [3] 609-14 (1990).
3. Y.-C. Zhou and M. N. Rahaman, "Hydrothermal Synthesis and Sintering of  $\text{CeO}_2$  Powders," J. Mater. Res., **8** [7] 1680-86 (1993).
4. R. Birringer, H. Gleiter, H.-P. Klein, and P. Marquard, "Nanocrystalline Materials: An Approach to a Novel Solid Structure with Gas-like Disorder," Phys. Lett., **102A** 365-69 (1984).
5. P. A. Badkar and J. E. Bailey, "The Mechanism of Simultaneous Sintering and Transformation in Alumina," J. Mater. Sci., **11** 1794-1806 (1976).
6. M. Kumagai and G. L. Messing, "Controlled Transformation and Sintering of a Boehmite Sol-Gel by  $\alpha$ -Alumina Seeding," J. Am. Ceram. Soc., **68** [9] 500-505 (1985).

## Figure Captions

- Fig. 1. Transmission electron micrograph of the  $\text{Al}_2\text{O}_3$  powder as received from the manufacturer. (Courtesy of M. Niu.)
- Fig. 2. Shrinkage ( $\Delta L/L_0$ ) and relative density ( $\rho$ ) of the  $\text{Al}_2\text{O}_3$  powder compact during sintering in air at  $10\text{ }^\circ\text{C}/\text{min}$  to  $1350\text{ }^\circ\text{C}$ .
- Fig. 3. X-ray diffraction patterns of the powder compact after heating at  $10\text{ }^\circ\text{C}/\text{min}$  to (a)  $1100\text{ }^\circ\text{C}$  and (b)  $1200\text{ }^\circ\text{C}$ . (The vertical lines correspond to the reference peaks of  $\alpha\text{-Al}_2\text{O}_3$ .)
- Fig. 4. Scanning electron micrographs of the fractured surfaces of the powder compacts after heating at  $10\text{ }^\circ\text{C}/\text{min}$  to (a)  $1100\text{ }^\circ\text{C}$ , (b)  $1200\text{ }^\circ\text{C}$ , and (c)  $1350\text{ }^\circ\text{C}$ .
- Fig. 5. Shrinkage ( $\Delta L/L_0$ ) versus temperature for the compacts formed from the powder heated rapidly to  $1300\text{ }^\circ\text{C}$  prior to compaction (a), the powder doped with  $\text{MgO}$  (c), and the powder seeded with fine  $\alpha\text{-Al}_2\text{O}_3$  particles (d). For comparison, the data for the compact formed from the as-received powder are also shown (b).

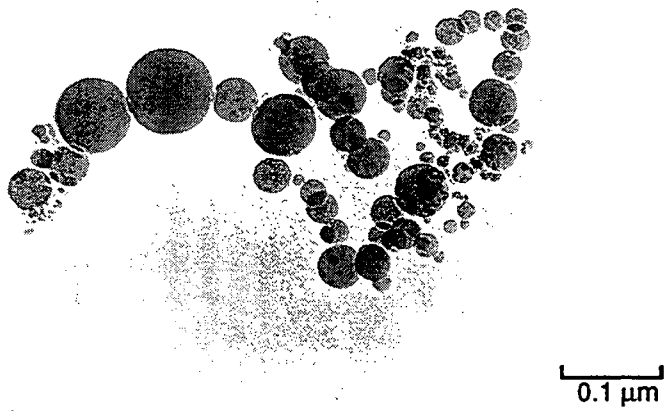


**Figure 1**

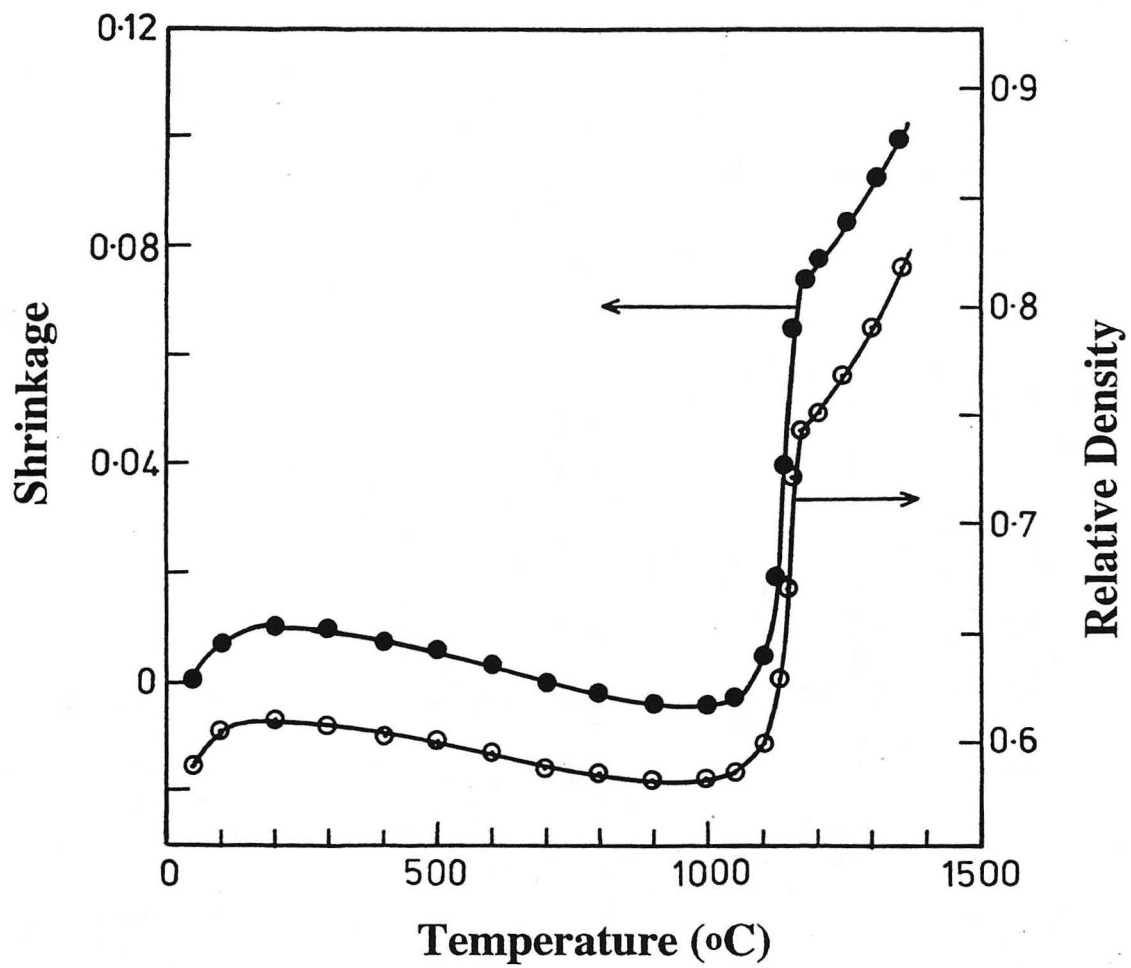


Figure 2

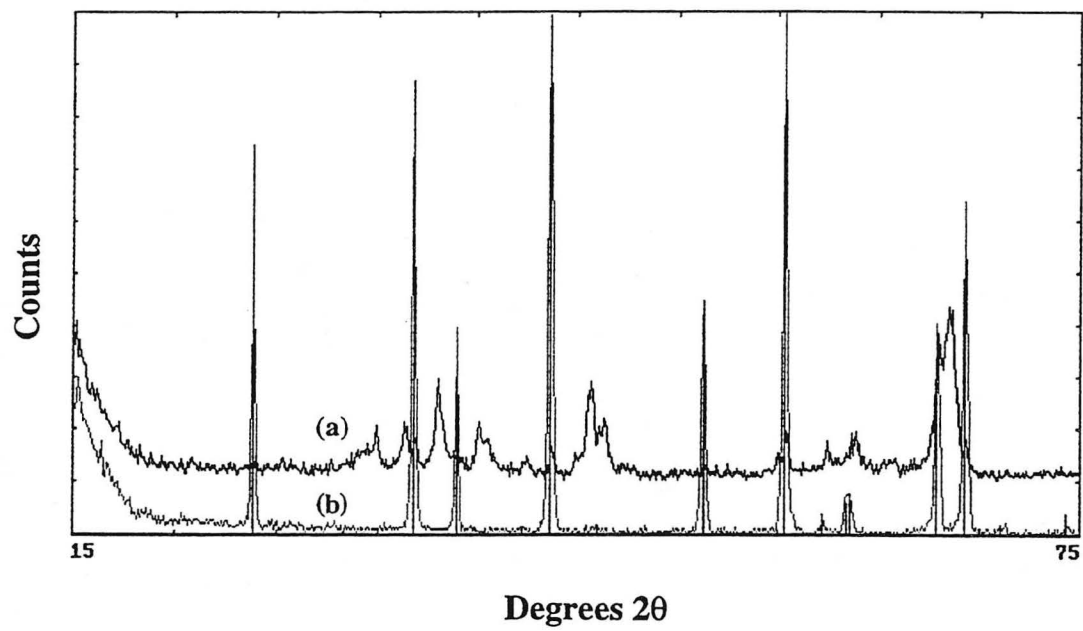


Figure 3

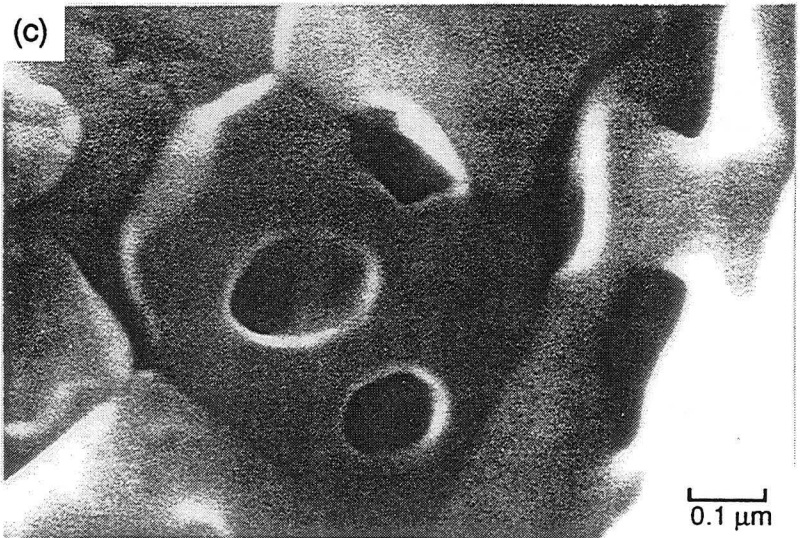
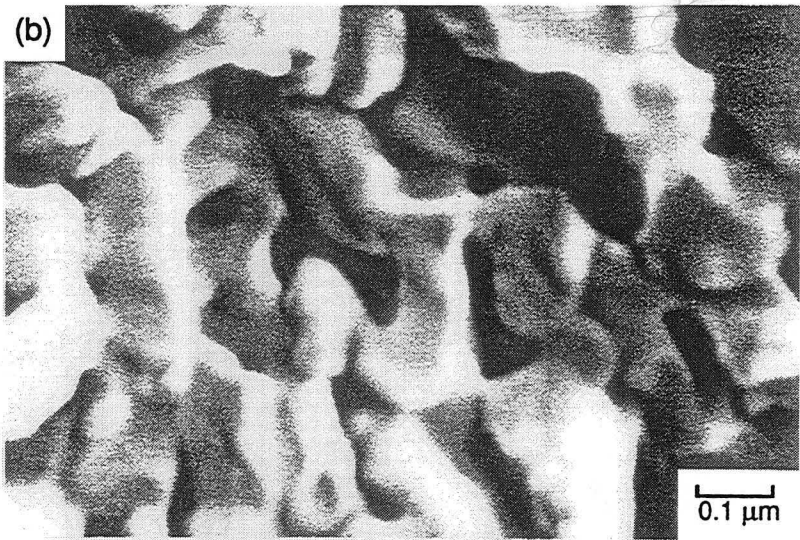
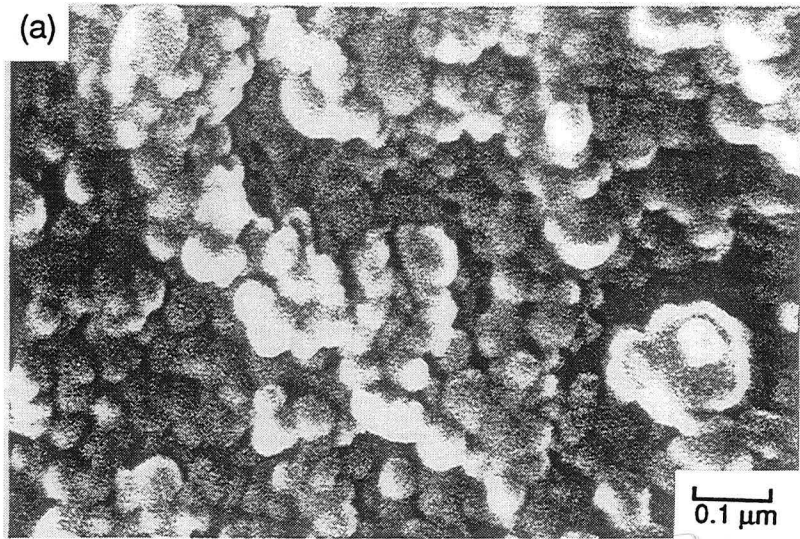


Figure 4

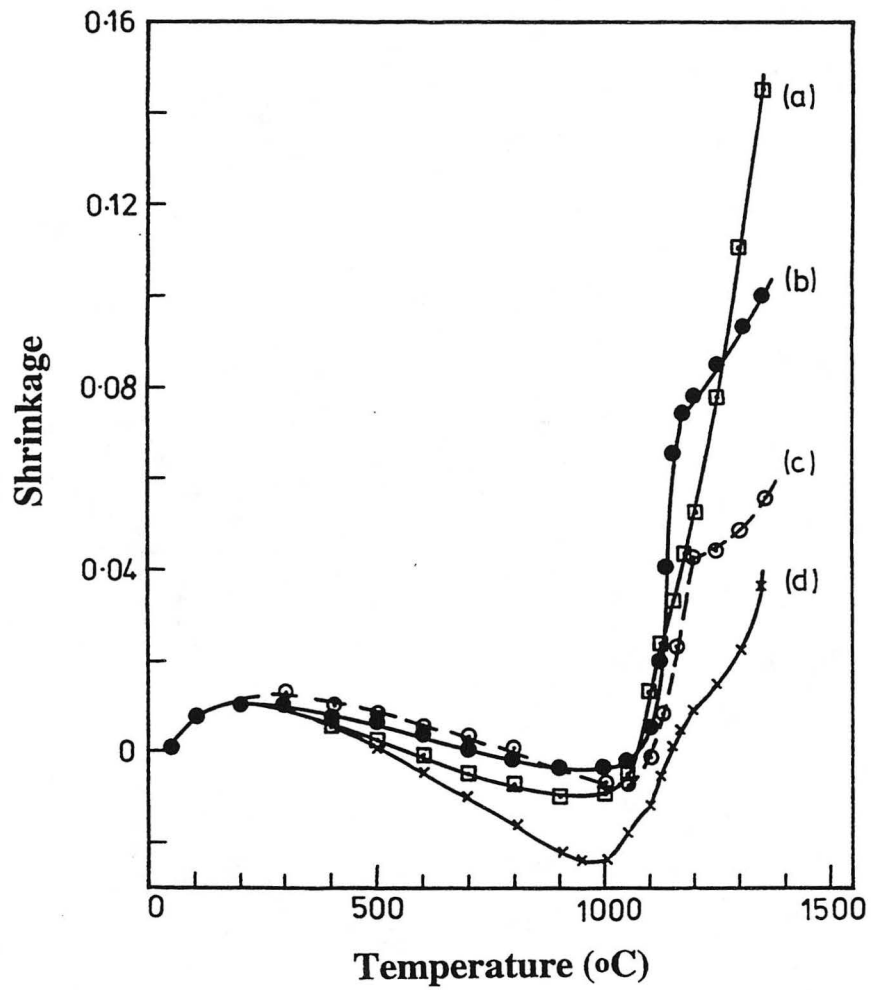


Figure 5

LAWRENCE BERKELEY LABORATORY  
UNIVERSITY OF CALIFORNIA  
TECHNICAL INFORMATION DEPARTMENT  
BERKELEY, CALIFORNIA 94720